Theor Chem Acc (2009) 123:127–135
DOI 10.1007/s00214-009-0550-z

REGULAR ARTICLE

Ion binding to polyelectrolytes: Monte Carlo simulations versus classical mean field theories

Sergio Madurga · Josep Lluís Garcés · Encarnació Companys · Carlos Rey-Castro · José Salvador · Josep Galceran · Eudald Vilaseca · Jaume Puy · Francesc Mas

Received: 13 February 2009 / Accepted: 16 February 2009 / Published online: 10 March 2009

Abstract The influence of ion size and surface charge model in titrations of ionizable polyelectrolytes is studied by means of the Semi Grand Canonical Monte Carlo simulation method in the context of the primitive model. Three models describing a discrete distribution of charged functional groups on the polyelectrolyte and different values for the radius of the background electrolyte spanning from ionic to hydrated radii values were analyzed. The polyelectrolyte titrations were simulated by calculating the degree of ionization versus pH curves at two ionic strengths. The results allow us to quantify the impact of the sizes of the background salt ions and surface functional groups of the polyelectrolyte on the dissociation degree. This influence is explained in terms of the effectiveness of the screening of the charged surface sites. Finally, by comparison with the Non-Linear Poisson–Boltzmann model, the influence of ionic correlations and finite size of the solution ions is assessed.

Keywords Macromolecular complexation · Polyelectrolytic effect · Specific binding · Monte Carlo simulation · Semi Grand Canonical · Non-Linear Poisson–Boltzmann theory

1 Introduction

Interactions of metal ions with natural complexants in aqueous media (small ligands, macromolecules and surfaces) play an important role in the bioavailability and toxicity of these elements. Figure 1 summarizes the possible interactions of a metal ion with soluble ligands, natural organic/inorganic colloids, biological surfaces and sediments in aqueous media [1, 2]. The study of these interactions is pertinent to several areas within environmental science: (a) biogeochemical cycles of the metal elements; (b) bioavailability and toxicity of the metal ions; (c) water treatment processes [3]. All these interactions can be schematized as

$$\mathrm{M}_{\mathrm{aq}}^{n_+} + (-\mathrm{L})_{\mathrm{aq/s}}^{z_-} \overset{K_{\mathrm{bin}}^{\mathrm{app}}}{\Leftrightarrow} (-\mathrm{LM})_{\mathrm{aq/s}}^{n_+ + z_-} \quad (1)$$

where –L represents a generic binding site.

In most cases –L does not behave as an ideal (homogeneous) ligand and the value of the apparent binding affinity, $K_{\mathrm{bin}}^{\mathrm{app}}$, is not a constant. Rather, $K_{\mathrm{bin}}^{\mathrm{app}}$ often depends on the metal concentration due to the presence of sites with different chemical functionalities, the presence of mutual interactions between sites, conformational changes in the macromolecule, aggregation processes, etc [1, 4, 5]. This fact is referred to as chemical heterogeneity. Moreover, both pH and ionic strength influence the net charge of the macromolecule/surface and modulate the electrostatic

Dedicated to Professor Santiago Olivella on the occasion of his 65th birthday and published as part of the Olivella Festschrift Issue.

S. Madurga · E. Vilaseca · F. Mas (✉)
Physical Chemistry Department, Research Institute of Theoretical and Computational Chemistry (IQTCUB), Barcelona University (UB), C/Martí i Franquès, 1, 08028 Barcelona, Spain
e-mail: fmas@ub.edu

J. L. Garcés · E. Companys · C. Rey-Castro · J. Salvador · J. Galceran · J. Puy
Chemistry Department, Lleida University (UdL), Av. Rovira Roure, 191, 25198 Lleida, Spain

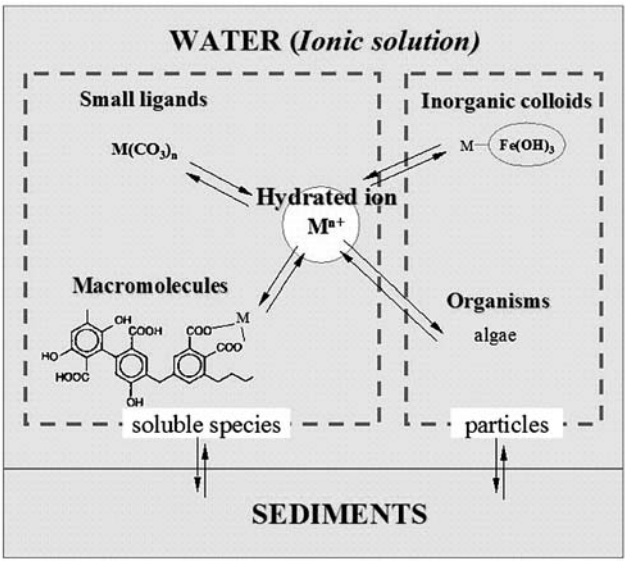

Fig. 1 Scheme of interactions of metal ions in aquatic natural system. Metal speciation includes free hydrated ion and inorganic and organic complexes. Adapted from [1]

interactions between cations and binding sites. This phenomenon is usually referred to as polyelectrolytic effect [2, 6]. The presence of inorganic cations other than M^{n+} (at least H^{+}), also modifies the effective binding energy of a given ion giving rise to competitive effects [7, 8].

Many efforts have been devoted to characterize the polyelectrolyte effect in the ion binding processes to natural complexants. Most of this work has been undertaken within the context of mean field theories, which allow the definition of the so-called surface potential. Once the surface potential is known, the electrostatic contribution to the binding energy and the specific binding can be straightforwardly obtained (see Sect. 2 for a detailed discussion).

Beyond mean field theories, considerable research has been addressed to characterize the distribution of ions [electric double layer (EDL)] around a charged surface, which is usually modelled as a continuous distribution of charge [see Ref. 9 and references quoted therein]. Just a few attempts have been made to include the discreteness of the surface charge or to discuss the approximations implicit in the integration of the Poisson equation when computing the potential profile of the EDL around a discretely charged flat surface [see Ref. 10 for a detailed discussion].

In order to study ion-ion correlations and the effect of finite ion size in the specific ion binding to polyelectrolyte surfaces, Monte Carlo (MC) simulation methods have been applied in recent years. Most previous works used a Grand Canonical Monte Carlo (GCMC) method where the interaction between the charged monomers of the polyelectrolyte is modelled by a Debye-Hückel potential influenced by the salt level [see Ref. 2 and references quoted therein]. Two examples are the study of the titration of polyelectrolytes, taken either as a rigid rod or as a freely joined chain [11] and the non-uniform charge distribution on annealed weakly charged polyelectrolytes [12].

Few attempts use Semi Grand Canonical Monte Carlo (SGCMC) simulations, combining a GCMC for the ion binding and a Canonical Monte Carlo (CMC) for the rest of the ions of the supporting electrolyte. The introduction of the CMC procedure allows the explicit description of the electrolyte solution, while the Grand Canonical formalism is needed to consider chemical reactions, such as protonation and deprotonation processes occurring when the polyelectrolytes have binding sites. The combination of both procedures allows a good description of the equilibrium between the charged polyelectrolyte and the electrolyte solution. Among the SGCMC simulations, we recall the interpretation of potentiometric titrations of carboxymethyl-cellulose in aqueous salt solutions [13, 14], and the role of electrostatic interactions in calmodulin–peptide complex formation [15]. Recently, Lund's group [16] has developed a Grand Canonical Titration Monte Carlo (GCTMC) method, similar to SGCMC method, but with a constant chemical potential restriction for the inert electrolytes. This method has been used to study the experimental and theoretical evidence of overcharging of calcium silicate hydrate within the primitive model in planar geometry. The main practical difference between both methods is that SGCMC fixes the bulk concentration of electrolyte ions, whereas GCMC method fixes their chemical potential. Thus, the latter method requires additional calculations to correlate the fixed chemical potential with concentration values. On the other hand, the number of electrolyte ions has to be significantly greater than the number of counterions in SGCMC, in order to ensure that the bulk electrolyte concentration is adequately simulated. Consequently, SGCMC simulations require, in general, more particles and larger systems than GCMC method. Therefore, GCMC will probably be the best choice for very diluted solutions, for which the size of the SGCMC simulation box would become excessively large. On the contrary, SGCMC method is more convenient for the simulation of concentrated solutions, as those studied here.

In this paper, we present SGCMC simulation results in the context of the primitive model, which represent, to our current knowledge, the first attempt to use SGCMC in planar geometry. The ions of the inert salt are modelled as charged hard spheres, the solvent is treated as a dielectric continuum, and the polyelectrolyte is represented as a discretely charged flat surface. In contrast to simple models that consider the charged wall as a surface with a continuous distribution of charge, in these simulations a discrete charge distribution was considered. Hence, the ionized functional groups were modelled as an array of charged

sites distributed on the surface. For the ions of the inert salt, different ion sizes are considered, from values representing the ionic radius to hydrated radii values. The comparison of the obtained results with hydrated and non-hydrated sizes allows us to discuss the effect of ions near the charged surface losing their solvation water molecules. In our simulations, proton binding to a discrete polyelectrolyte charge distribution is studied using a Grand Canonical Monte Carlo procedure coupled to a Canonical MC algorithm that describes the electrolyte solution. The probability of binding depends on both the pH and the intrinsic stability constant, K_0. The SGCMC results in planar geometry shown here are aimed at simulating the experimental titrations curves of a typical latex particle [17]. Typically, latex particles are spherical particles with a radius of hundreds of nm. Thus, a surface complexation model using planar geometry could be adequate to rationalize the polyelectrolytic effect of this kind of systems.

The organization of the paper is as follows. In Sect. 2 (theoretical background), we summarize previous approaches within the mean field theories. Section 3 is devoted to the SGCMC simulation method. Within this context, we discuss the dependence of the dissociation degree versus pH curve on the size of the ions of the inert salt and the impact of three different models of surface charge distribution. Moreover, the calculation of an approximate average surface potential is discussed as well as its dependence on the pH. This potential is compared with that obtained within the classical Non-Linear Poisson Boltzmann (NLPB) treatment.

2 Theoretical background

For the sake of simplicity, we will restrict ourselves to the proton binding to polyelectrolytes. Acid–base equilibrium of polyions is generally described by Henderson–Hasselbach equation

$$pK_{\mathrm{dis}}^{\mathrm{app}} = \log K_{\mathrm{bin}}^{\mathrm{app}} = \mathrm{pH} - \log\left(\frac{\alpha}{1-\alpha}\right) \tag{2}$$

where $K_{\mathrm{dis}}^{\mathrm{app}} = \left(K_{\mathrm{bin}}^{\mathrm{app}}\right)^{-1}$ labels the apparent dissociation constant of the polyacid and α is the degree of dissociation.

In terms of the proton coverage $\theta = 1 - \alpha$, or the charge, Q, of the polyacid, $\theta = (Q_{\max} - Q)/Q_{\max}$, Eq. 2 can be rewritten as

$$pK_{\mathrm{dis}}^{\mathrm{app}} = \mathrm{pH} + \log\left(\frac{\theta}{1-\theta}\right) = \mathrm{pH} + \log\left(\frac{Q_{\max} - Q}{Q}\right) \tag{3}$$

where $Q_{\max}$ is the maximum charge in the fully deprotonated macromolecule [6].

Two components of free energy have been recognized in the proton binding affinity: one from electrostatic origin, written as $F\psi_{\mathrm{S}}$ and giving rise to the electrostatic binding, and a second one of chemical origin, $-RT \ln K_{\mathrm{c}}$, responsible for the specific binding [1, 6]. Within the mean field approximation, ψ_{S} is the average (surface) electrostatic potential close to the binding sites with respect to the bulk solution, F is the Faraday constant, R is the ideal gas constant and T the temperature.

Then, the apparent dissociation/binding constant can be factorized as

$$pK_{\mathrm{dis}}^{\mathrm{app}} = \log K_{\mathrm{bin}}^{\mathrm{app}} = \log K_{\mathrm{c}} - \frac{1}{\ln 10}\tilde{\psi}_{\mathrm{S}}; \quad \tilde{\psi}_{\mathrm{S}} \equiv \frac{F\psi_{\mathrm{S}}}{RT} \tag{4}$$

where K_{c} is the so-called average equilibrium function [1, 4]. K_{c} measures the chemical or specific binding affinity

$$\log K_{\mathrm{c}} = pH_{\mathrm{S}} + \log\left(\frac{1-\alpha}{\alpha}\right) = pH_{\mathrm{S}} + \log\left(\frac{Q_{\max} - Q}{Q}\right) \tag{5}$$

where $\mathrm{pH_S} = -\log c_{H_{\mathrm{S}}}$ labels the concentration of protons in a volume element close to the surface. This concentration is related to the bulk concentration by the Boltzmann distribution:

$$c_{H_{\mathrm{S}}} = c_H e^{-\tilde{\psi}_{\mathrm{S}}} \tag{6}$$

Notice that for a homogeneous polyelectrolyte, the average equilibrium function, K_{c}, defined in Eq. 5, usually becomes a constant, which we refer to as the intrinsic stability constant, K_0.

In order to characterize the electrostatic binding, the master curve procedure [18, 19] consists in plotting the experimental results in terms of the surface pH ($\mathrm{pH_S}$) and obtaining a representation independent of the ionic strength, i.e.,

$$Q = f(\mathrm{pH}, I) = f'(\mathrm{pH_S}) \tag{7}$$

The macromolecular ligands can be classified according to their characteristic dimension: (a) *nanometer-scale*: characteristic length $\delta \sim$ (1–10) nm; (b) *interfacial regions*: thickness $\delta \sim (10\text{–}10^3)$ nm. Examples of ligands of the first kind are: synthetic soluble polyelectrolytes (e.g., polyacrylic acid), humic and fulvic acids, etc., and for the second kind are: microorganisms, organic-coated sediments, cell walls in seaweeds, etc.

A physical picture of the charge distribution of the systems of the first kind consists in a set of fixed charges distributed over a region of space partially accessible to solvent and salt ions (Fig. 2a). In the c*ylindrical/spherical models* the charges are homogeneously distributed (smeared-out) within an impermeable rod/sphere of radius $r \sim \delta$, creating around an electrostatic field of cylindrical/spherical symmetry. The charge-potential relationship within a mean field approximation can be easily estimated using the Poisson-Boltzmann equation [6, 20, 21]. Another

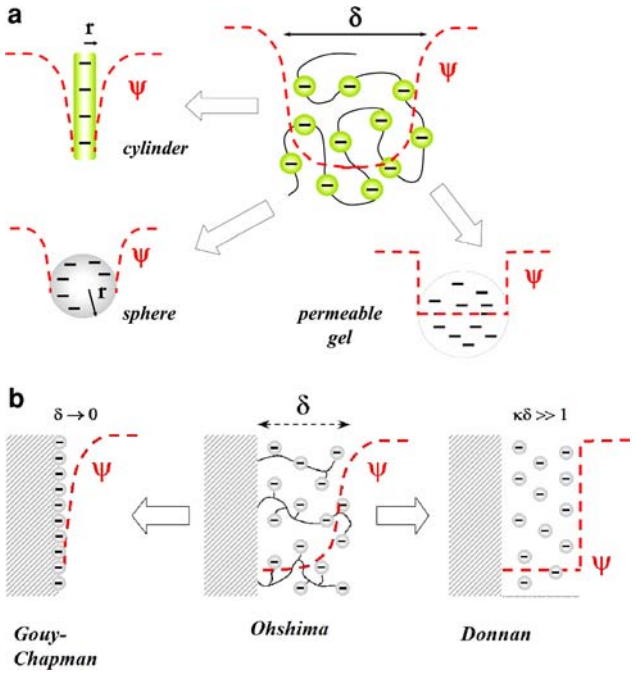

Fig. 2 **a** Common electrostatic models used for macromolecules [6, 10], **b** common electrostatic models used for surfaces [14]. κ is the inverse of the Debye length

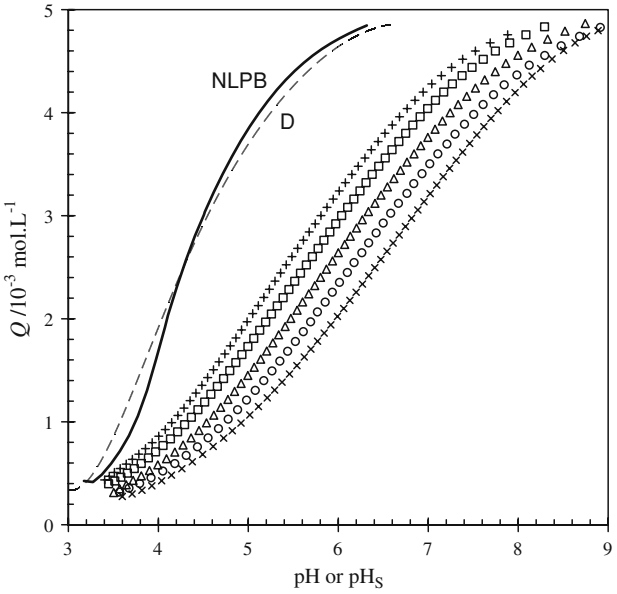

Fig. 3 Experimental Q vs. pH data of the PAA titrations. Markers $I = 0.1$ M (*plus symbol*), 0.05 M (*triangle*), 0.02 M (*square*), 0.01 M (*circle*), 0.005 M (*multi symbol*). "Master curve", Q vs. pH_S, obtained solving the NLPB equation in cylindrical geometry with $r = 0.55$ nm (labelled NLPB *continuous line*) and applying the Donnan model (labelled D *dashed line*). Adapted from [6]

approximation (schematized in the lower rightmost part of Fig. 2a) is to use the *permeable gel (Donnan)* model which assumes that the colloid behaves as an electroneutral, permeable gel phase with a uniform potential [6, 22].

On the other hand, most of the systems of the second kind can be regarded as "soft particles" [23], having a charged layer of thickness δ, partially permeable to solvent and mobile ions, where the metal complexation processes occur. Again, this charge distribution can be approximated by simplified models, using either NLPB in flat geometry or Donnan model, as depicted in Fig. 2b.

In all previous models, the main problem is usually the estimation of a geometric parameter (δ, specific area, volume of Donnan phase, spherical or cylindrical radius, etc.), which, due to the crude approximations assumed it is often regarded as an empirical parameter. Just as an example, Fig. 3 shows the proton binding results to the polyacrylic acid (PAA) [6, 24], where the radius of the cylinder is optimized. Experimental Q versus pH curves converge into a Q versus pH_S master curve by numerically solving the NLPB equation (assuming cylindrical geometry) or by using the Donnan model [see details in Ref. 6].

So, although similar master curves can be obtained with different mean field descriptions, sometimes—even within the same model—the master curve is not unique and the resulted fitted parameters differ between models and from independent direct experimental measures. This suggests that the fitting process might mitigate the effects of the crude assumptions involved in each treatment, e.g., the oversimplified geometry, the absence of ion–ion correlations and finite ion size effects, etc.

3 SGCMC simulations

3.1 Model and simulation procedure

The equilibrium properties of the ionic solution in contact with the charged surface (where binding processes occur) were obtained through Monte Carlo computer simulations performed in the Semi Grand Canonical ensemble (SGCMC) at a temperature of 300 K. The solution was modelled as a collection of N_+ positive ions and N_- negative ions confined in a rectangular prism of dimensions $W \times W \times L$. The square charged wall was situated at $z = 0$. This wall and the opposite one at $z = L$ were treated as impenetrable to ion displacements. On the contrary, periodic boundary conditions and the minimum image convention [9, 10] were employed in the x and y directions. The values of N_+ and N_- were selected according to the concentration of the bulk electrolyte solution as indicated below. A suitable concentration of counterions was also added to neutralize the surface charge.

Ions were treated as charged hard spheres having radius values, a, of 0.2 (average ionic radius), 0.3 and 0.36 nm (average hydrated radius). The radius value of 0.36 nm is a

mean value of the hydrated radii of typical monovalent ions such as Na^+ and Cl^- [10, 25]. The 0.2 value was considered in order to take into account that ions near the charged surface lose their solvation water molecules. On the other hand, solvent molecules (water) were not explicitly considered, but its dielectric constant was used in the ion–ion interaction energy expressions. The interaction energy between two charges Z_i and Z_j separated by a distance r can be formulated as

$$\begin{cases} u(\vec{r}) = \dfrac{Z_i Z_j e^2}{4\pi\varepsilon r}; & r \geq d \\ u(\vec{r}) = \infty; & r < d \end{cases} \tag{8}$$

where d is the sum of the ionic radii of the two particles ($d = 2a$), ε is the permitivity of the dielectric continuum, and e is the elementary charge. The method of Boda et al. was implemented to correct the effects of truncating long-range interactions [10, 25–27].

The charged wall represents a distribution of ionizable functional groups on a colloidal interface. Its dimensions were kept fixed at 10.62×10.62 nm^2 in all the simulations and the ionizable functional groups were modelled as an array of 169 (13×13) charged sites. Thus, adjacent sites were separated by a distance of 0.82 nm, given a maximum surface charge density of -0.24 Cm^{-2}, which is a typical value of many interfaces with ionizable carboxylate groups [2]. The surface site-ion interaction energy has been calculated as in the ion–ion case. The third dimension of the simulation box (L) was scaled according to the ionic strength and total number of ions in bulk solution, being always greater than 50.0 nm. Ionic strengths of 0.1 and 0.01 M were considered, whereas the total number of ions in bulk solution ranged between 700 and 1,400, depending on the pH value.

Three models have been considered to represent the structure of the surface charges (Fig. 4): DISC1, DISC2 and DISC3. In DISC1 model, the sites are point charges situated at the surface plane. In DISC2 model, the sites are charged hard spheres with a finite radius of 0.3 nm whose centres are also situated at the surface. The value of 0.3 nm corresponds to the estimated non-hydrated radius of the carboxylate functional group [15]. In DISC3 model, the sites are charged hard spheres with a finite radius of 0.1 nm whose centres are located 0.2 nm above the surface. The radius of 0.1 nm has been chosen as an approximation to the radius of the charged atom in a carboxylate functional group.

When simulating a titration experiment of the polyelectrolyte in presence of an inert salt at constant ionic strength and a given pH, the protons are not explicitly considered in the simulations of the electrolyte solution.

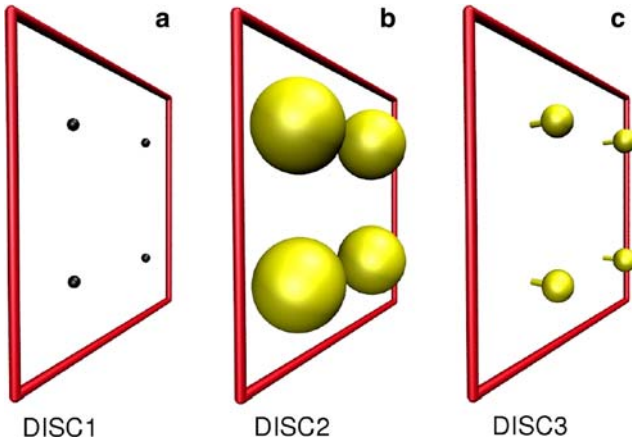

Fig. 4 Schematic representation of the three models for the surface charge distribution used in MC simulations: **a** discrete distribution of point charge sites over the surface (DISC1 model), **b** discrete distribution of spherical charge sites of radius 0.30 nm over the surface (DISC2 model), and **c** discrete distribution of charge sites outside the surface (DISC3 model)

Rather, they are substituted by counterions, as done in other simulation studies [13, 14, 16]. Moreover, in order to keep the global electroneutrality of the system, we added the same number of counterions as the initial number of charged surface sites considered.

The use of the SGCMC method [13, 14] allows the charged surface sites to be in equilibrium with an electrolyte solution. In this model, ions can move and surface sites can change their charge status via a protonation (neutralization) or a deprotonation (charging) process. This surface charge variation is accompanied with annihilation or creation of a counterion in the electrolyte solution to maintain the electroneutrality of the system. According to the protonation processes depicted in Eq. 1, the Monte Carlo test energy can be expressed in terms of the free energy change, ΔF:

$$\begin{cases} \Delta F = \Delta U_{\mathrm{el}} + k_{\mathrm{B}} T (\ln 10)(\mathrm{pH} - \log K_0) \\ \qquad \text{for protonation process} \\ \Delta F = \Delta U_{\mathrm{el}} - k_{\mathrm{B}} T (\ln 10)(\mathrm{pH} - \log K_0); \\ \qquad \text{for deprotonation process} \end{cases} \tag{9}$$

where ΔU_{el} is the change in electrostatic energy due to the addition or the deletion of charges. For the intrinsic equilibrium protonation/deprotonation constant of the surface-charged sites, a value of $\log\left(K_0/\mathrm{M}^{-1}\right) = 4.41$ was considered, which corresponds to the intrinsic stability constant of protonation of a generic carboxylic functional group [6]. The simulations were performed using a code developed in C under LINUX operating system in a 36 CPU cluster.

3.2 Calculations and results

Titration curves showing the dependence of the degree of dissociation, α, on the pH were calculated for the different ionic strengths, ionic radii and surface charge models (Figs. 5, 6).

For DISC1 surface model, the titration curve in 0.1 M salt solution using three different ionic radii (0.20, 0.30 and 0.36 nm) is shown in Fig. 5a. From the comparison of the three profiles obtained with SGCMC simulations, an important effect of the ion radius on the degree of dissociation can be observed. For a fixed pH, the values of α increase as the radius of the background electrolyte decreases. This can be explained as the surface charges being more easily screened by smaller ions and facilitating higher dissociation degrees.

Continuous line in Fig. 5a also shows the plot of α versus pH obtained using the mean field PB approximation. Combining Eqs. 2, 4 and 6 for a homogeneous polyelectrolyte, with $K_c = K_0$, and $\tilde{\psi}_S$ computed by solving the NLPB theory for a flat surface [6, 23], we obtain the following expression

$$\theta = (1-\alpha) = \frac{K_0 c_H e^{-\tilde{\psi}_S}}{1 + K_0 c_H e^{-\tilde{\psi}_S}} = \frac{K_0 c_{H_S}}{1 + K_0 c_{H_S}} \tag{10}$$

which is a Langmuir isotherm in terms of the surface proton concentration. At most fixed pH values, PB approach overestimates the value of the degree of dissociation with respect to the simulation data. This result is consistent with the fact that SGCMC predicts higher α for smaller ions, since PB model is the limiting case of point charges. For pH lower than pK_0, however, SGCMC simulations yield values of α which are slightly larger than the ones predicted for PB theory. Although the relative error of these α values could explain this effect, it seems to be a systematic feature in all the simulations performed. One possible explanation of this phenomenon could be a local effect of accumulation of counterions near every surface charge site, which induces an inversion of the sign of the actual surface potential, so that the proton binding becomes less favoured compared to what happens in mean field approximations. This phenomenon can be seen as a local overcharging process, which disappears if we average the local ionic concentration profiles over the surface (in terms of x and y). Moreover, this effect would be more significant at low surface charge density, due to the fact that only few surface functional groups are charged. This effect is larger for smaller ionic radii, as can be seen in Fig. 5a for pH values lower than the actual pK_0, since more ions can approach the surface.

The titration curve at 0.01 M with DISC1 surface model is shown in Fig. 5b. As in 0.1 M solution, an important impact of the ionic radius on the degree of surface charge

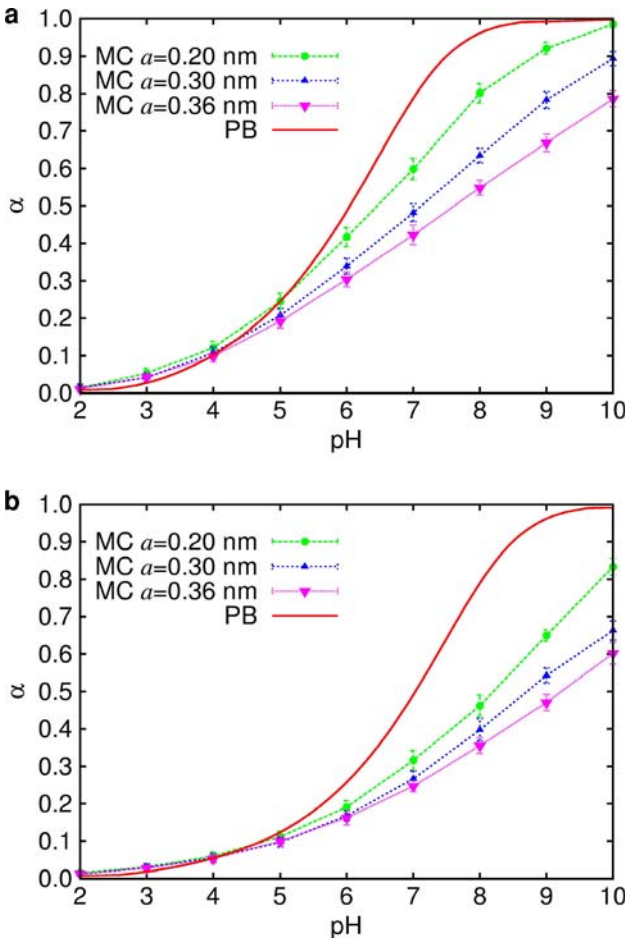

Fig. 5 Comparison between PB (*continuous line*) and SGCMC simulations (DISC1 model) of the degree of dissociation (α) as a function of pH for 0.20 nm (*circle*), 0.30 nm (*triangle*) and 0.36 nm (*inverted triangle*) ion radii at $I = 0.1$ M (**a**), and 0.01 M (**b**)

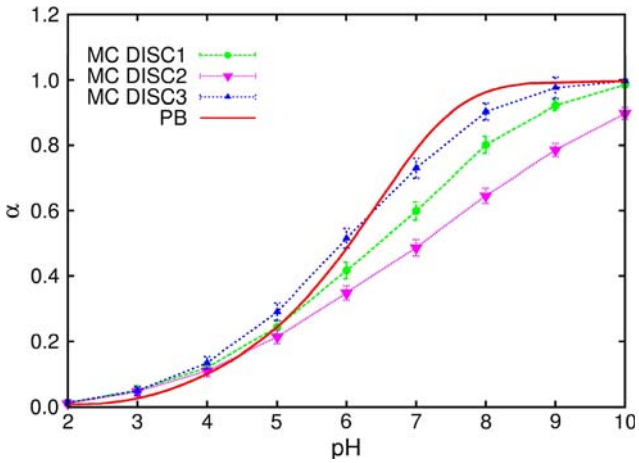

Fig. 6 Comparison between PB (*continuous line*) and SGCMC simulations with DISC1 (*circle*), DISC2 (*inverted triangle*) and DISC3 (*triangle*) surface models for the degree of dissociation (α) as a function of pH for $a = 0.20$ nm in 0.1 M salt solution

can be observed. The SGCMC curves for the three ion radii at 0.01 M show lower degrees of surface ionization than the corresponding curves at 0.1 M. The repulsive interaction between negatively charged surface sites are now less screened by a lower ionic strength (from 0.1 to 0.01 M), which hinders the deprotonation (ionization) of the sites, and accordingly lower surface charge values are obtained. On the other hand, at low pH values (lower than the actual pK_0 value), the effect explained above (values of the degree of dissociation higher than the ones predicted by PB mean field approximation) is less pronounced. This can also be due to the lower screening of the surface charges by the background ions and, consequently, to the more negative surface potential compared to higher ionic strength, which makes the local overcharging phenomena less favoured.

Notice that only the titration curve at the lowest radius seems to approach a sigmoidal behaviour similar to what is observed in experimental data of, e.g., PAA titrations (Fig. 3) or also in titration experiments of latex particles [17].

To further investigate the effect of the screening of the charged surface sites by the ionic medium, a comparison with two additional models, DISC2 and DISC3 was also performed. In this case, a value of 0.2 nm for the radius of the solution ions was considered. This comparison is shown in Fig. 6. Notice that the α values obtained in DISC2 model fall below those of DISC1 model in the whole pH range. In DISC2, the large volume of the surface sites causes a steric effect that hinders the solution ions from approaching the surface as close as in DISC1 model. Consequently, the surface-charged sites are less screened. In DISC3 model, however, the sites are separated from the surface, although they display a smaller radius in order to render a size value for the whole functional group similar to the one chosen for DISC2 model. Therefore, in the DISC3 case a larger number of ions can approach the surface and screen its charge more effectively, yielding a larger α. In fact, the α values obtained for the DISC3 surface model lie above those of DISC1 model, within the whole studied range of pH (Fig. 6). This can be explained as DISC3 model allowing a higher local surface concentration of counterions near a surface-charged site, compared with the other two models, which also yields higher values of the dissociation degree at low pH values, as explained above.

From the behaviour of the surface models considered in this study, we conclude that the shape of the α versus pH curve is strongly dependent on the geometric representation of the surface functional groups. Within the three surface models considered in this study, DISC3 model is the best one to reproduce the sigmoidal shape of the experimental curves, as discussed above, probably due to the fact that the surface functional group is more realistically represented in this model that in the others. This fact suggests that, apart from the size of the inert salt ions, also the size of the charged functional groups and their location with respect to the surface are crucial in order to obtain realistic titration curves to be compared with experimental data.

Finally, in order to test the accuracy of the mean field approximation for the derivation of a master curve from experimental titration data, it is interesting to compare the average electrostatic surface potential, ψ_S. This potential is the only parameter in mean field approximation theories that takes into account all the electrostatic interactions and the distribution of the surface charges. This average surface potential can be estimated, within MC simulations, by using

$$\psi(z) = \frac{1}{N_{z_{\max}}} \sum_{j=1}^{N_{z_{\max}}} \left\{ \frac{1}{N_{\text{conf}}} \sum_{i=1}^{N_{\text{conf}}} \frac{e}{\varepsilon W^2} \times \left(\sum_{k=1}^{N_{\text{ions}}} (z - z_k) Z_k \right)_i ; \quad z_k \le z_{\max,j} \right\} \tag{11}$$

at the distance of maximum approach for the ions of the inert electrolyte to the polyelectrolyte surface, which in our case, is the average ionic radius, i.e., $\psi_S = \psi(z = a)$. This expression gives the profile of the electrostatic potential along the z coordinate (normal to the charged surface). As the discrete distribution of charge in the surface causes a dependence of the ion density in the x and y directions, this z profile is obtained, in a first approximation, as an average along those directions. The expression used is similar to that obtained from integration of the Poisson equation for a continuously charged flat surface [see Eq. 6 in Ref. 10], but averaging over the N_{conf} Monte Carlo configurations and for the $N_{z_{\max}}$ different values of the maximum distance $z_{\max}$, from which it is reasonable to suppose bulk conditions. Ten different values of $z_{\max}$ around half of the length of the simulation box of W^2 surface area were selected. For each value of $z_{\max}$ chosen, 5000 MC ionic configurations were used to calculate an estimation of the electrostatic potential. The inner summation is extended over all k ions, N_{ions}, with $z_k \le z_{\max,j}$ independently of the x_k, y_k values, being $z_{\max,j}$ the maximum distance chosen in each case. As the dependence on x and y is neglected, the obtained value can be seen as an approximate mean electrostatic potential.

In Fig. 7, the surface potential as a function of pH is analyzed for PB and SGCMC simulations of DISC1, DISC2 and DISC3 surface models with a radius of 0.2 nm for the solution ions. In all models, we obtain surface potential values at low pH values that are slightly more negative with respect to PB prediction, corresponding to slightly higher values of the surface charge density and slightly higher values of the degree of dissociation (Fig. 6).

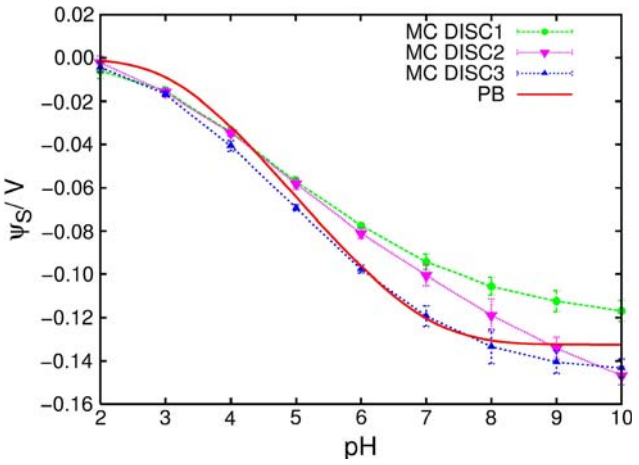

Fig. 7 Approximate surface potential of polyelectrolyte for $a = 0.20$ nm in 0.1 M salt solution and of varying pH and simulation model [DISC1 (*circle*), DISC2 (*inverted triangle*) and DISC3 (*triangle*)]. PB results are also included—in *continuous line*—for comparison purposes

In contrast, at high surface charge and, consequently, high pH values, less negative surface potential values are obtained with respect to PB. This is consistent with the lower values of the degree of dissociation obtained from SGCMC simulation with respect to PB prediction (Fig. 6). However, DISC2 model yields values of the surface potential more negative than those given by DISC1 model, in apparent contradiction with the lower values of the degree of dissociation previously described in DISC2 model. This behaviour can be explained from the approximate potential profiles predicted by the three surface models, which are shown in Fig. 8. Notice that, for a particular pH value (e.g., pH = 8), DISC2 model yields values of the potential that are more negative than the ones obtain from DISC1 model. This might be due to the poor definition of the surface potential, since in all models we have chosen the value at the position of maximum approach for the ions ($z = a$), but this is not sufficiently accurate for DISC2 surface model due to the large excluded volume close to the surface. For this model, a better definition of the surface potential consists in taking $z = 2a$ as the distance of maximum approach. With this definition, the value of the surface potential obtained form DISC2 model will be less negative than the one obtained from DISC1 model, which is consistent with the behaviour of the degree of dissociation shown in Fig. 6.

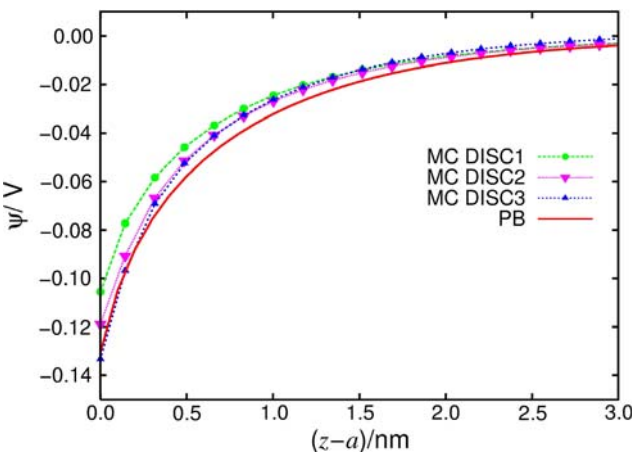

Fig. 8 Electrostatic potential as a function of surface distance for $a = 0.20$ nm in 0.1 M salt solution and pH = 8, for three simulation models [DISC1 (*circle*), DISC2 (*inverted triangle*) and DISC3 (*triangle*)]. PB results are also included—in *continuous line*—for comparison purposes

Figure 8 also shows that the potential profiles differ close to the surface, but they tend to merge when moving a few atomic radii towards the bulk solution. Moreover, the potential profile obtained from PB mean field approximation approaches that obtained from DISC3 model near the surface and only separates slightly at intermediate distances. This fact explains why DISC3 model displays the best agreement with PB predictions and warns us about the difficulty in the definition of an average surface potential.

4 Conclusions

An SGCMC simulation method was applied to the study of an ionizable polyelectrolytic surface with planar geometry in equilibrium with an aqueous salt solution described by a primitive model. The effects of ion size and surface charge characteristics on the proton titration curves have been analyzed. Although the primitive model is probably not accurate enough for the quantitative reproduction of experimental results, due to its excessive simplicity, the present approach is still valuable for the elucidation of the most appropriated simulation conditions. The cases considered in this work suggest that the most appropriate model to represent the surface charge distribution is DISC3 and that the best choice for the ion size could be the average ionic radius of the ions in solution (0.2 nm). Under these conditions, the titration curve resembles the sigmoidal wave displayed by experimental data better. Moreover, these simulation conditions allow us to estimate an approximate value for the average electrostatic surface potential which is not very different from the one predicted by PB mean field theory. This potential was able to fit experimental titration data of polyelectrolytes in presence of monovalent salt solutions at moderate concentrations with good accuracy.

Acknowledgments The authors gratefully acknowledge support of this research by the Spanish Ministry of Science and Technology (Projects UNBA05-33-001, CTM2006-13583 and CTQ2006-14385)

and from the "Comissionat d'Universitats i Recerca de la Generalitat de Catalunya".

References

1. Buffle J (1998) Complexation reactions in aquatic systems: an analytical approach. Ellis Horwood, Chichester
2. Borkovec M, Jönsson B, Koper GJM (2001) In: Matijevic E (ed) Surface and colloid science, vol 16. Kluwer, New York
3. Rey-Castro C, Lodeiro P, Herrero R, De Vicente MES (2003) Environ Sci Technol 37:5159. doi:10.1021/es0343353
4. Garcés JL, Mas F, Puy J, Galceran J, Salvador J (1998) J Chem Soc 94:2783. doi:10.1039/a803558j
5. Garcés JL, Mas F, Cecília J, Companys E, Galceran J, Salvador J, Puy J (2002) Phys Chem Chem Phys 4:3764. doi:10.1039/b201345m
6. Companys E, Garcés JL, Salvador J, Galceran J, Puy J, Mas F (2007) Colloid Surf A 306:2. doi:10.1016/j.colsurfa.2007.01.016
7. Rusch U, Borkovec M, Daicic J, Riemsdijk WH (1997) J Colloid Interface Sci 191:247. doi:10.1006/jcis.1997.4904
8. Garcés JL, Mas F, Puy J (2004) J Chem Phys 120:9266. doi:10.1063/1.1710857
9. Quesada-Pérez M, González-Tovar E, Martín-Molina A, Lozada-Casou M, Hidalgo-Álvaez R (2003) Chem Phys Chem 4:234. doi:10.1002/cphc.200390040
10. Madurga S, Martín-Molina A, Vilaseca E, Mas F, Quesada M (2007) J Chem Phys 126:234703. doi:10.1063/1.2741520
11. Ullner M, Jönsson B (1996) Macromolecules 29:6645. doi:10.1021/ma960309w
12. Zito T, Seidel C (2002) Eur Phys J E 8:339. doi:10.1140/epje/i2002-10019-y
13. Nishio T (1994) Biophys Chem 49:201. doi:10.1016/0301-4622(93)E0070-L
14. Nishio T (1996) Biophys Chem 57:261. doi:10.1016/0301-4622(95)00057-3
15. André I, Kesvatera T, Jönsson B, Åkerfeldt KS, Linse S (2004) Biophys J 87:1929. doi:10.1529/biophysj.104.040998
16. Labbez C, Nonat A, Pochard I, Jönsson B (2007) J Colloid Interface Sci 309:303. doi:10.1016/j.jcis.2007.02.048
17. Cakara D, Chassagne C, Gehin-Delval C, Borkovec M (2007) Colloid Surf A 294:174. doi:10.1016/j.colsurfa.2006.08.006
18. Wit JCM, Riemsdijk WH, Koopal LK (1993) Environ Sci Technol 27:2005. doi:10.1021/es00047a004
19. Kinniburgh DG, Riemsdijk WH, Koopal LK, Borkovec M, Benedetti MF, Avena MJ (1999) Colloids Surf A 151:147. doi:10.1016/S0927-7757(98)00637-2
20. Anderson CF, Record MT (1990) Annu Rev Biophys Chem 19:423. doi:10.1146/annurev.bb.19.060190.002231
21. Sharp KA, Honig B (1990) Annu Rev Biophys Chem 19:301. doi:10.1146/annurev.bb.19.060190.001505
22. Miyajima T (1995) In: Marinsky JA, Marcus Y (eds) Ion exchange and solvent extraction. Marcel Dekker, New York
23. Ohshima H (1998) In: Ohshima H, Furusawa K (eds) Electrical phenomena at interfaces. Fundamentals, measurements and applications. Marcel Dekker, New York
24. Nagasawa M, Murase T, Kondo K (1965) J Phys Chem 69:4005. doi:10.1021/j100895a060
25. Quesada-Pérez M, Martín-Molina A, Hidalgo-Álvarez R (2004) J Chem Phys 121:8618. doi:10.1063/1.1798932
26. Boda D, Chan KY, Henderson D (1998) J Chem Phys 109:7362. doi:10.1063/1.477342
27. Boda D, Fawcett WR, Henderson D, Sokolowski S (2002) J Chem Phys 116:7170. doi:10.1063/1.1464826